

VALIDATION OF EQUIBIAXIAL FLEXURAL TEST FOR MINIATURIZED CERAMIC SPECIMENS

— S. Kondo, Y. Katoh, J.W. Kim, L.L. Snead (Oak Ridge National Laboratory)

OBJECTIVE

The objective of this work is to develop a mechanical test technique which can utilize very small volume specimens of ceramic materials, is free from a strong effect of edge flaw, and can be applied to elevated temperature testing in addition to room temperature testing.

SUMMARY

For the purpose of evaluating fracture strength of irradiated ceramic specimens, a miniature disc equibiaxial flexural test technique was developed. It was applied to graphite specimens in a variety of combination of sample thickness and loading ring diameter to investigate the influences on the stress uniformity within the loading ring. Although similar and relatively high Weibull modulus were observed for all conditions ($m \approx 20$), the significant stress concentration associated with the large deflection was observed at the loading location for thinner specimens ($t < 0.2\text{mm}$). However, the true local fracture stress was successfully estimated from the measured fracture load using finite element analysis. The method for estimating true local fracture stress appear reasonable for evaluating the fracture strength of dense poly-crystalline graphite, and can be used for determination of the statistical parameters for fracture stress of various ceramics.

PROGRESS AND STATUS

Introduction

For determination of fracture strength of neutron-irradiated monolithic ceramics and graphite materials, four-point flexural test is most commonly employed. Uni-axial flexural tests such as those in four-point and three-point configurations are simple and readily applicable to elevated temperature tests. However, these tests require specimens with substantial volumes, typically several cubic centimeters per specimen, for standard dimensions defined in various test standards. On the other hand, due to the statistical nature of ceramic strength, a set of data usually requires sample population of typically 30, making the total volume of samples required to produce statistically significant data difficult using the standard specimens. In order to avoid this difficulty, miniaturized flexural specimen geometries and dimensions are often employed in neutron irradiation studies.^[1] However, such experiments frequently suffer from modification to the statistical strength due to edge flaws which have been introduced during specimen handling in hot cells and are very difficult to evaluate in a quantitative manner.

Among the alternative methods to the miniaturized uni-axial flexural tests, the equibiaxial flexural testing is a promising technique capable of 1) testing a specimen even smaller than the miniaturized flexural specimens, 2) applying a surface equibiaxial tensile loading onto a sample, 3) testing in a simple and robust manner, making post-irradiation evaluation fairly easy, 4) producing statistically significant data from a small volume neutron irradiation experiment, and 5) readily applicable to elevated temperature testing. Furthermore, the measurement of the strength of brittle materials under bi-axial flexure conditions rather than uniaxial flexure is often considered more reliable, because the maximum tensile stresses occur within the central loading area and spurious edge failures are eliminated. The objective of this work is to develop such an equibiaxial disc flexural test for strength determination of ceramic and graphite materials. In a previous report, ^[2] authors demonstrated that such a test technique developed is effective to determine the apparent flexural strength of thin specimen of pyrocarbon. However, the correction factor for estimating true local stress at the location of fracture origin, where the stress concentration is anticipated, from the apparent stress may be essential. The present work is intended to determine the influences of the sample thickness and loading ring diameter on the flexural strength using dummy graphite samples in an attempt to estimate the true local fracture stress at the location of fracture origin.

Experimental Procedure

The equibiaxial flexural test in a “ring-on-ring” configuration, where a disc specimen of ceramics is placed on a support ring and loaded with a smaller diameter coaxial loading ring, was adopted as a method of strength

evaluation at ambient temperature. This test method is often utilized for equibiaxial strength of brittle ceramics and the test procedure is standardized in ASTM C1499-05. [3]

A typical disc equibiaxial flexural test utilizes ceramic specimens of diameter of the order of one inch. However, because the evaluation of miniature samples requires testing using much smaller dimensions, a dedicated fixture was designed and fabricated. The section view of the test setup is shown in Fig. 1 and in a set of photographs in Fig. 2. The physical parameters of the test configuration and the condition of testing are summarized in Table 1.

Dummy specimens used were near-isotropic poly-crystalline nuclear graphite (AXF-5Q produced by Poco-Graphite Inc., TX, USA). Dimensions of the disc specimens were 6.0 mm (diameter) \times 0.10, 0.15, and 0.20 mm (thickness). Whereas, only the tension side was polished by 6 mm diamond plate for most DL251T150 (see the notation in Table 1) using Minimet 1000 (Buehler Ltd., IL, USA), both surfaces of discs for DL116T100, DL116T150, DL116T350, DL251T100, L251T200, and L251T350 were polished in the same manner.

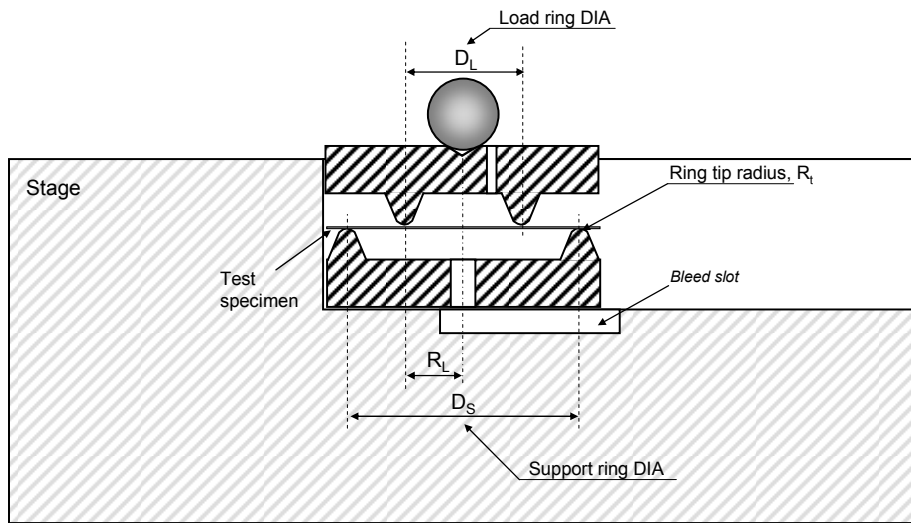


Fig. 1: Section view of the equibiaxial flexural test configuration.

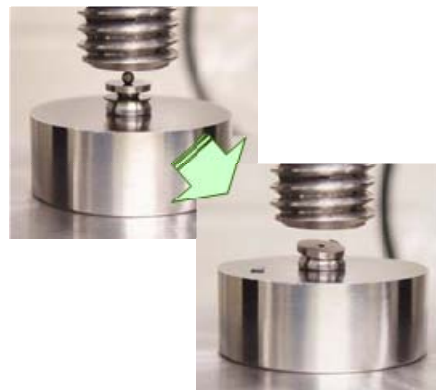


Fig. 2: Photographs of test specimen and fixture before (top-left) and after (bottom-right) testing.

Table 1: Physical parameters and condition of the tests.

Sample IDs	Loading Ring DIA. D_L [mm]	Avg. Sample Thickness t [mm]	Std. Dev. for t [mm]	Number of Specimens Tested [pcs.]
DL116T100	1.16	0.101	0.003	28
DL116T150	1.16	0.150	0.002	28
DL116T350	1.16	0.350	0.002	30
DL251T100	2.51	0.101	0.003	28
DL251T150	2.51	0.152	0.004	29
DL251T200	2.51	0.200	0.003	28
DL251T350	2.51	0.349	0.003	30

Estimation of true local stress

Results of the ring-on-ring tests for graphite thin discs ($t \leq 0.2$ mm) are summarized in Table 2. The load-displacement curves show large deflection (see displacement to thickness ratios in Table 2; $d/t = 1.3$ -2.5) and non-linear load-displacement relationship as presented in Fig. 3. Such deviation from linear elastic theory have been previously observed in ring-on-ring testing for glass plate [4], and are associated with the reinforcing effect of outer overhang ($r > D_s$) which can not move freely toward the center. The displacements seem to depend on the loading ring diameter rather than the sample thickness. The failure patterns clearly indicate the stress magnification at the loading location as shown in Fig. 4. In the case of using the loading ring of smaller diameter ($D_L = 1.16$ mm), some fracture origins are likely located in the area just inside the loading ring. In order to quantitatively evaluate the location of fracture origin, the ratios of r_f to R_L were evaluated in this work, where the r_f is the radial distance between the likely crack origin and the disc center, the R_L is the loading ring radius. The mean r_f to R_L ratios were estimated to be 0.90 for $t = 0.1$ mm discs and 0.88 for $t = 0.15$ mm discs, indicating the fracture origin just inside the inner ring. For the tests with larger load ring ($D_L = 2.51$ mm), the r_f/R_L ratios show higher values ($r_f/R_L = 0.92$ -0.95) compared to smaller load ring case, indicating much significant localized stress near the loading location.

Table 2: Summary of results of ring-on-ring test for thin graphite discs.

Sample IDs	Avg. Displacement	Avg. Fracture Load	Mean Fracture Origin	Weibull Mean Local Stress ¹⁾	Std. Dev. for $\sigma_{p,max}$	Weibull Modulus
	d [mm]	F [N]	r_f/R_L	$\sigma_{p,max}$ [MPa]	[MPa]	m
DL116T100	0.252	3.13	0.90	134	9.16	18.1
DL116T150	0.259	5.23	0.88	143	9.42	18.8
DL251T100	0.239	5.62	0.95	127	8.61	18.3
DL251T150	0.229	8.79	0.92	126	10.4	14.8
DL251T200	0.226	13.6	0.94	133	8.49	19.5

1) Local flexural stresses were estimated from fracture load by finite element method.

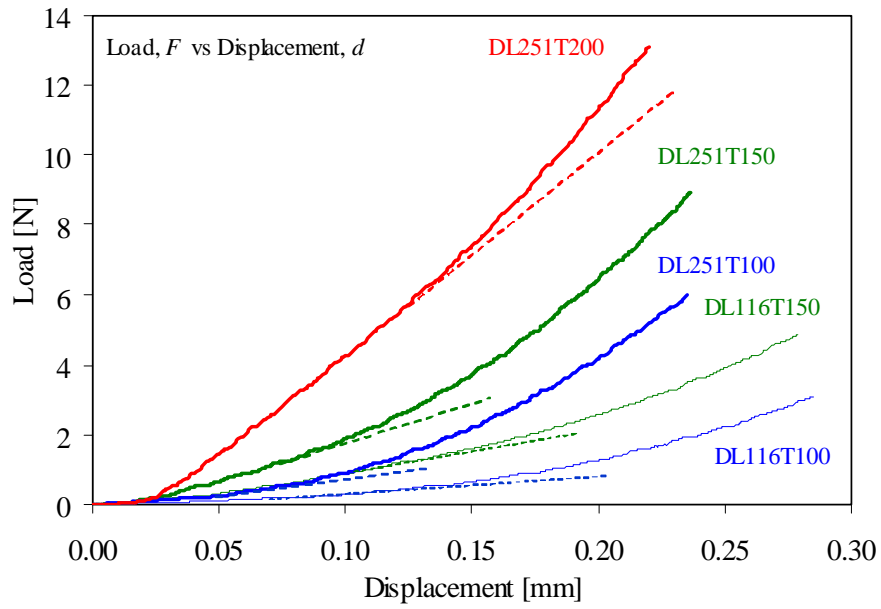


Fig. 3: Typical load-displacement curve for thin disc samples.

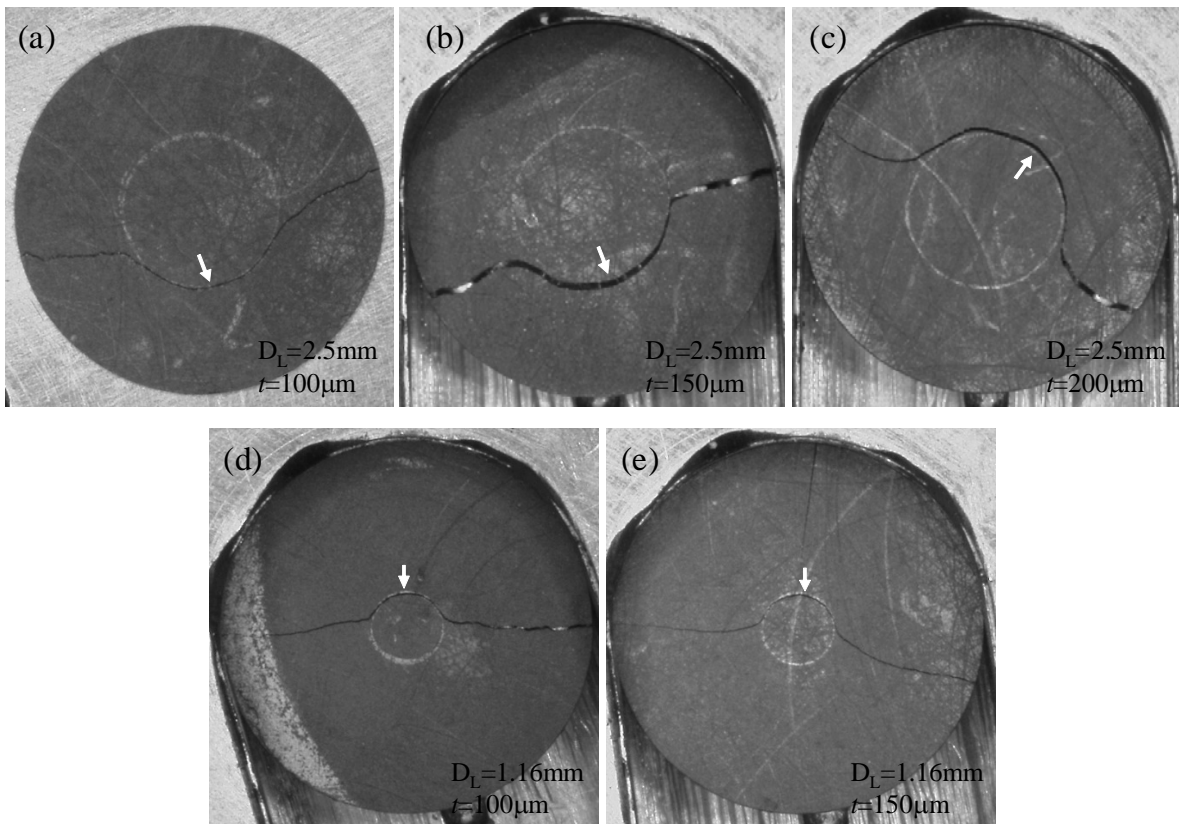


Fig. 4: Failure patterns of graphite discs tested by loading ring with $D_L=2.51$ for $t=$; (a) 100, (b) 150, (c) 200 μm , or $D_L=1.16\text{mm}$ for $t=$; (d) 100, (e) 150 μm . Likely fracture origins are indicated by arrows (viewed from compression sides for clear vision of loading ring trace).

Kao et al. reported that stress magnification at the loading point is significant when the plate deflection exceeds one-half the specimen thickness [5]. In that case, the equibiaxial stress calculation following ASTM 1499-05 may not be utilized to relate the flexural strength to the flexural load. The local stress at the loading location in a ring-on-ring configuration has been empirically and analytically approximated considering the ratio of deflection to specimen thickness in an attempt to solve the nonlinear plate equations [5,6]. However, these valuable solutions have no application to thin graphite samples because of the significant deviation from Hooke's law or elastic-plastic fracture behavior. Therefore, finite element analysis was employed in this study to estimate the true local stress from the applied load. Figure 5 shows the radial stress distribution in the ring-on-ring loading for the same material and experimental conditions as Table 1. The stress magnifications beneath (or near) the loading point are computationally well demonstrated by the finite element analysis. The local stress at the loading point is estimated to be twice as large as that at disc center for the $t=100\ \mu\text{m}$, $D_L=2.51\ \text{mm}$ case. For smaller loading ring case ($t=100\ \mu\text{m}$, $D_L=1.16\ \text{mm}$), somewhat more uniform stress distribution is observed, where the maximum stress is about 1.3 times larger than the center stress. Therefore, one can conclude that the fracture load is governed primarily by the local stress associated with the significant curvature at the loading point in all cases tested.

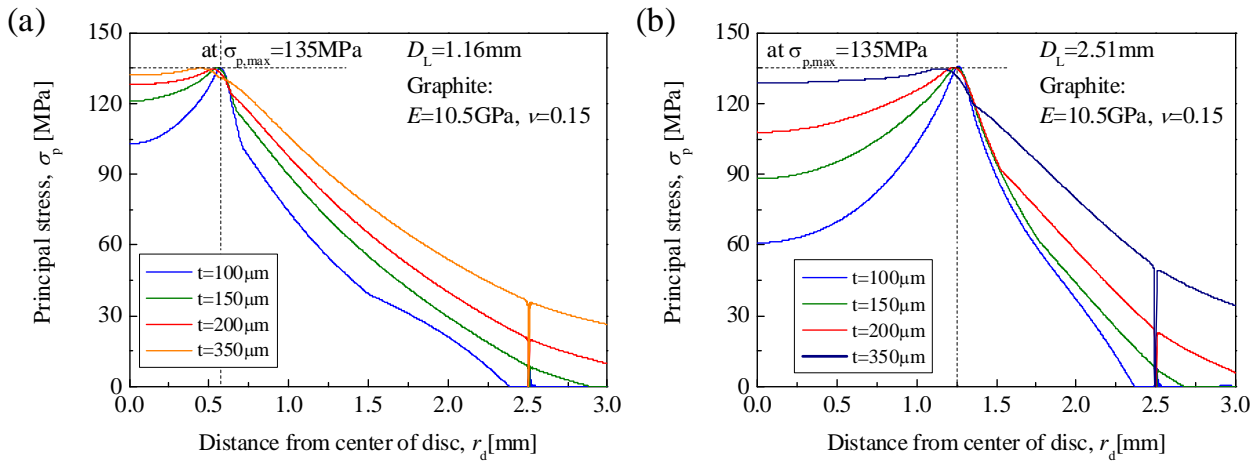


Fig. 5: Radial stress distribution at an approximate flexure stress at the loading location (~135MPa) analyzed by finite element method.

Figure 6 shows the Weibull statistical plots of the flexural strength of graphite discs, where the true local stress at the loading point was estimated from the fracture load using finite element calculation. The Weibull mean strengths are summarized in Table 2. Although strength were not widely scattered for each case, slight higher strength for using $D_L=1.16\ \text{mm}$ case ($\sigma_f=134, 143\ \text{MPa}$) than the $D_L=2.51\ \text{mm}$ case ($\sigma_f=127-133\ \text{MPa}$) was observed. All the measured fracture strength are higher than the commercially reported flexural strength of 86 MPa (standard four-point flexural test [7]) and the typical reported value of 113 MPa for small size bend specimens ($2.3 \times 6 \times 30\ \text{mm}$ [8]). For most ceramics, strength depends on the effective stressed area or volume because of the statistical distribution of strength-controlling flaws such as machining flaws [9]. The limited effective-stressed area might modify the results of the present work, though no consistent relationship between bi-axial and uni-axial flexural strength data has been established [10,11]. It is worth noting that the similar and relatively high Weibull modulus ($m=18.1-19.5$) for each test set except for DL251T150 ($m=14.8$) were observed. The slight smaller Weibull modulus for DL251T150 is possibly due to the variety of the roughness for the as machined compressive surface and/or the presence of the residual stress at there.

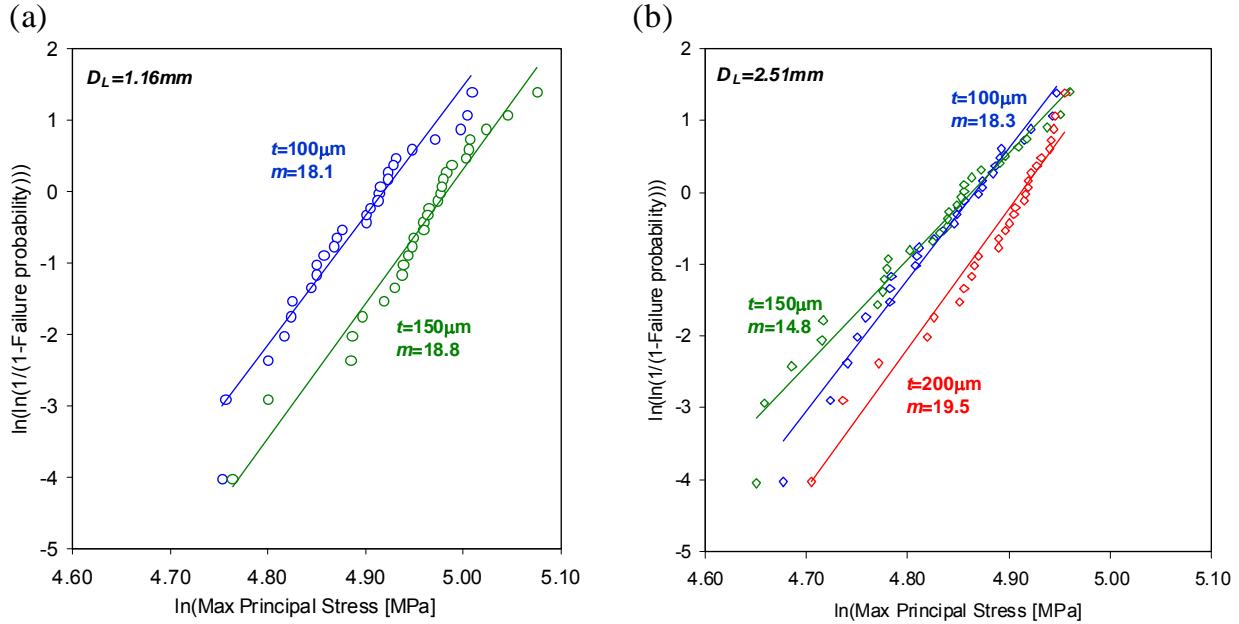


Fig. 6: Weibull distribution of flexural strength of graphite specimens with different thickness tested by loading ring with diameter of ; (a) $D_L = 1.16\text{mm}$, (b) $D_L = 2.51\text{mm}$.

Comparison with result from thicker samples

Results of the ring-on-ring tests for thick graphite discs ($t=0.35\text{ mm}$) are summarized in Table 3. The load-displacement curve shows relatively small displacement to thickness ratio ($d/t=0.55-0.64$) and non-linear load-displacement relationship at $d > \sim 0.1\text{ mm}$ as presented in Fig. 7. The direction of deviation from the linear load-displacement is opposite of the thinner disc cases. It is well known that strain-stress curve of graphite both in uni-axis static tensile and compressive condition show a non-linear curve due to the decrease in Young's modulus [12]. Therefore, the reinforcing effect of the overhang is insignificant to such an extent that the deviation hide behind the intrinsic degradation of Young's modulus for the cases of thick samples. Figure 8 shows the typical failure patterns of the thicker discs for using the load ring with $D_L = 1.16\text{ mm}$ and $D_L = 2.51\text{ mm}$, respectively. Although, the likely fracture origins, which are indicated by arrows in Fig. 8, are located within inner ring contact lines for both loading ring cases, the flaw characteristics are significantly different. The crack was frequently deflected along the inner side of the load ring for $D_L = 2.51\text{ mm}$ case, whereas the approximately-straight cracks are seen in the $D_L = 1.16\text{ mm}$ case. As listed in Table 3, the mean r_i/R_L ratio for the case of using larger load-ring is three times larger than the smaller load-ring case. The much larger r_i/R_L ratio of 0.6 for DL251T350 may be attributed to the stress magnification that is still remaining inside the inner ring. Because the indirect crack growth normally increases the fracture energy, relatively higher strength might be observed for the $D_L = 2.51\text{ mm}$ case. Indeed, the strength of DL251T350 was clearly higher than that of the others in spite of the anticipated larger effective stressed area. The very limited reinforcing effects and near uniform stress distributions in a smaller loading ring configuration also observed in our FE analysis for thicker samples. From the both experimental and FE analysis results, the equibiaxial strength is confidently determined to be $129 \pm 7.8\text{ MPa}$ for graphite with the identical surface condition.

Table 3: Summary of results of ring-on-ring test for thick graphite discs.

Sample	Avg. Displacement d [mm]	Avg. Flexure Load F [N]	Mean Fracture Origin r_f/R_L	Weibull Mean Flexural Stress σ_f [MPa]	Std. Dev. for σ_f [MPa]	Weibull Modulus m
DL116T350	0.191	16.8	0.22	129	7.80	20.7
DL251T350	0.224	35.5	0.76	143	6.60	27.3

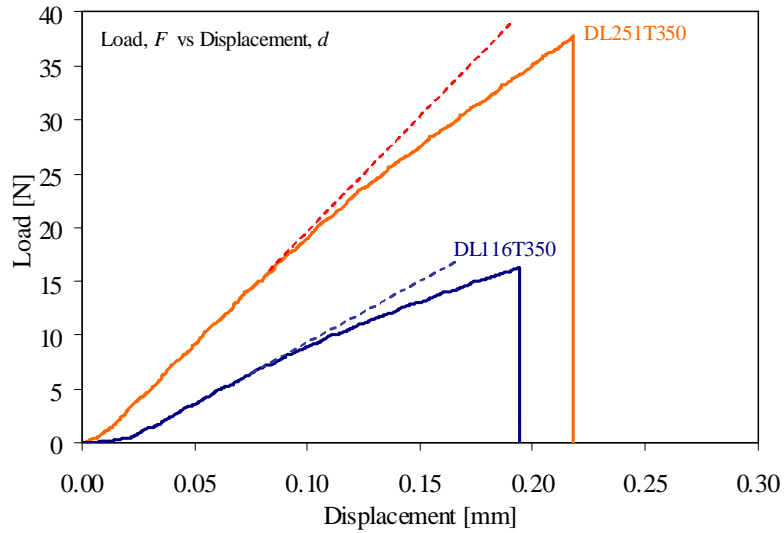


Fig. 7: Typical load-displacement curve for thin disc samples.

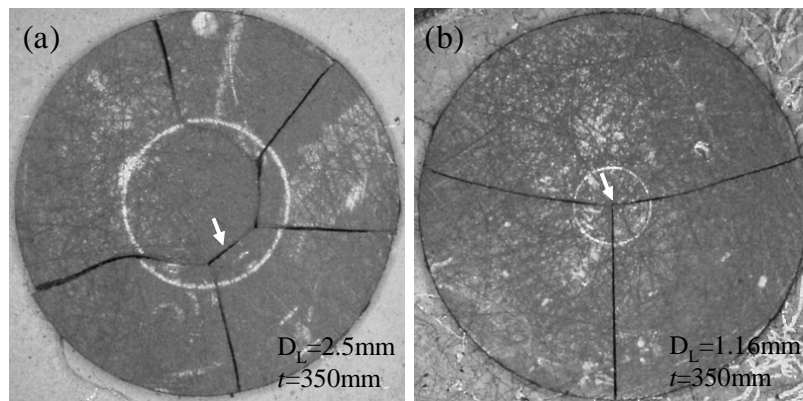


Fig. 8: Failure patterns of graphite discs tested by loading ring in the condition of; (a) $D_L=2.51$ mm $t=350$ μ m, (b) $D_L=1.16$ mm, 350 μ m. Likely fracture origins are indicated by arrows (viewed from compression sides for clear vision of loading ring trace).

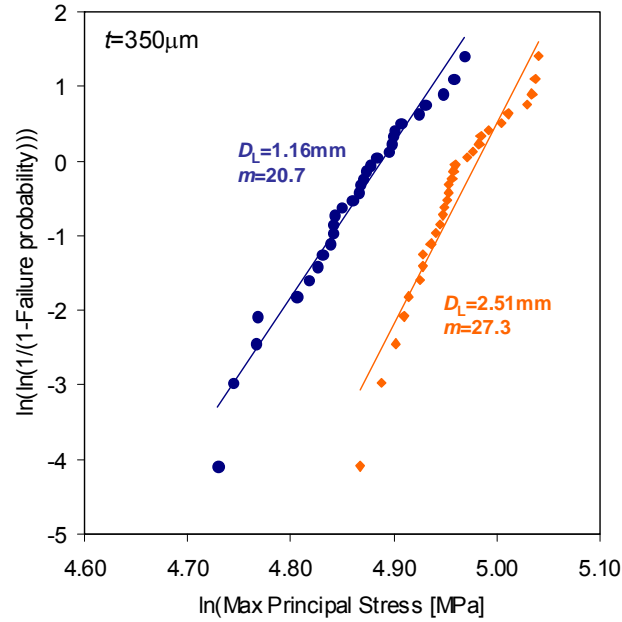


Fig. 9: Weibull distribution of equibiaxial strength of graphite specimens.

Figure 9 shows the Weibull statistical plots of the equibiaxial strength of graphite discs, where assuming principal stresses are uniform within the inner ring and estimated following eq. (7) in ASTM 1499-05 [2]. Although the reason for the slight smaller magnitude of Weibull modulus for DL116T350 ($m = 20.7$) is not clear, it is similar to the average m value for the test series of thinner discs. This is indicative that a single flaw type is responsible for the failure primarily due to the successful elimination of the edge failure. In this case, a simple methodology is used to convert the strength obtained with one test geometry to strength representing another test geometry: [13],

$$\frac{\sigma_1}{\sigma_2} = \left(\frac{S_1^{\text{eff}}}{S_2^{\text{eff}}} \right)^{-\frac{1}{m}} \quad (1)$$

where the subscripts 1 and 2 denote two different geometries of test specimens or configuration, S^{eff} is the effective surface area, m is the surface flaw controlling Weibull modulus. Particularly with small size specimen, the effect of stressed surface or volume on failure probability must be considered in order to extrapolate the measured strength to the strength of full size components. Figure 10 shows the flexural strength as a function of effective surface area for all test sets. The effective surface area were estimated based on the results of r_f/R_L ratio evaluation, where the uniform stress were assumed to be ranging from the loading point to lower limit of the standard deviation of r_f/R_L ratio. The slope of the linear-regression fitted line (loading length regressed on strength in this instance) is $-1/m$, which leads to an additional estimate of the Weibull modulus as 23.1. The additional Weibull modulus is slight larger than the m values obtained from results of each test sets, but it is still comparable to those results, which implies that the total area of stress magnified region may modify the apparent strength due to the size effect. Furthermore, the successfully scaled m value implies that Weibull material parameters such as characteristic strength and scale parameter can be certainly estimated from the ring-on-ring test results for high E/σ materials like PyC.

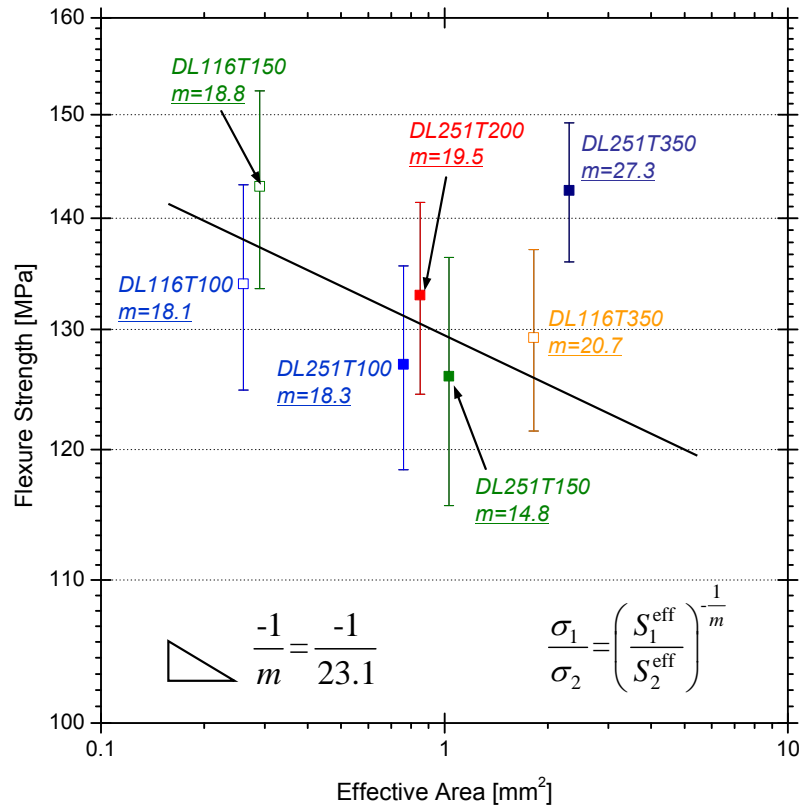


Fig. 10: Flexural strength versus effective surface area for specimens with different thickness.

References

- [1] L.L. Snead, T. Hinoki, Y. Katoh, "Strength of neutron irradiated silicon carbide and silicon carbide composite," Fusion Materials, ORNL/TM-2008/164, 49 (2002).
- [2] ASTM Standard C1499-05, "Standard Test Method for Monotonic Equibiaxial Flexural Strength of Advanced Ceramics at Ambient Temperature," ASTM International, West Conshohocken, PA.
- [3] R. Kao, N. Perrone, and W. Capps, "Large-Deflection Solution of the Coaxial-Ring-Circular-Glass-Plate Flexure Problem," J. Am. Ceram. Soc., 54,566-571 (1971).
- [4] J.B. Wacgman Jr., W. Capps, J. Mandel, Biaxial Flexure Tests of Ceramic Substrates, J. Mater. 7, 188-194 (1972).
- [5] J. Malzbender, R.W. Steinbrech, "Fracture test of thin sheet electrolytes for solid oxide fuel cells," J. Euro. Ceram. Soc. 27, 2597-2603 (2007).
- [6] POCO Graphite, Inc., Decatur, TX. <http://www.poco.com/>
- [7] L.L. Snead, T.D. Burchell, A.L. Qualls, Strength of Neutron-Irradiated High-Quality 3D carbon fiber composite, J. Nucl. Mater 321, 165-169 (2003).
- [8] J. Lamon, A.G. Evans, Statistical Analysis of Bending Strengths for Brittle Solids: A Multiaxial Fracture Problem, J. Am. Ceram. Soc. 66, 177-182 (1990).
- [9] M.N. Giovan, G. Sines, "Biaxial and Uniaxial Data for Statistical Comparison of a Ceramics's Strength," J. Am. Ceram. Soc., 52, 510-515 (1979).
- [10] D.K. Shetty, A.R. Rosenfield, W.H. Duckworth, P.R. Held, "A Biaxial-Flexure Test for Evaluating Ceramics Strength," J. Am. Ceram. Soc., 66, 36-42 (1983).
- [11] S. Yoda, M. Eto, T. Oku, Change in dynamic young's modulus of nuclear-grade isotropic graphite during tensile and compressive stressing, J. Nucl. Mater., 119, 278-283 (1983).
- [12] ASTM Standard C1683-08, "Standard Practice for Size Scaling of Tensile Strength Using Weibull Statistics for Advanced Ceramics," ASTM International, West Conshohocken, PA.